

Glomerular Hemodynamics in Established Glycerol-induced Acute Renal Failure in the Rat

Allen I. Wolfert and Donald E. Oken

Departments of Medicine, Medical College of Virginia; and Veterans Administration Hospital, Richmond, Virginia 23298-0160

Abstract

The glomerular dynamic correlates of failed filtration were studied in volume replete rats with established glycerol-induced acute renal failure (ARF). Over one-half of all nephrons formed virtually no filtrate, while the single nephron glomerular filtration rate (SNGFR) of fluid-filled nephrons, measured at the glomerulotubular junction to preclude the possibility of covert tubular leakage, averaged one-sixth of control ($P < 0.001$). Even that low mean value was elevated by a few nephrons with a near normal SNGFR. Renal failure thus reflected both total filtration failure in the majority of nephrons and massively reduced filtration in most of the remainder. Glomerular capillary pressure (P_g) averaged some 14 mmHg below control ($P < 0.001$), whereas the arterial colloid osmotic and Bowman's space pressures were not significantly altered. Renocortical and whole kidney blood flow were also unchanged. Marked internephron functional heterogeneity precluded estimates of the ultrafiltration coefficient. However, the fall in SNGFR correlated well with the markedly depressed P_g and afferent net filtration pressure (ΔP_{netA} , $P < 0.001$), which in turn were caused by increased preglomerular resistance and a reciprocal fall in efferent arteriolar resistance. This complex change in intrarenal resistances was largely, if not entirely, responsible for failed filtration in this ARF model.

Introduction

Various experimental models have been used as surrogates for studies of human acute renal failure (ARF)¹ (e.g., 1–7). Standard micropuncture techniques have yielded valuable information in each of these models, but this approach does not provide insight into the basic mechanisms responsible for the

Address reprint requests to Dr. Donald E. Oken, Medical College of Virginia, Box 160, MCV Station, Richmond, VA 23298-0160.

Dr. Wolfert's present address is Allegheny General Hospital, Pittsburgh, PA.

Received for publication 2 March 1989 and in revised form 12 June 1989.

1. *Abbreviations used in this paper:* ARF, acute renal failure; BW, body weight; CBF, cortical blood flow; COP_A , arterial colloid osmotic pressure; cs, centistoke; ΔP_{netA} , net afferent filtration pressure; ΔP_{net} , mean net filtration pressure; GBF_A , afferent glomerular blood flow; GBF_E , efferent glomerular blood flow; GFR, whole animal filtration rate; GTJ, glomero-tubular junction; Hct, hematocrit; LG, lissamine green; LGTT, lissamine green transit time; MAP, mean arterial pressure; P_{BS} , Bowman's space pressure; P_g , glomerular capillary pressure; P_{sf} , stop flow pressure; P_{star} , star vessel pressure; P_t , proximal tubule pressure; R_A , preglomerular vascular resistance; R_E , postglomerular vascular resistance; SNFF, single nephron filtration fraction.

The Journal of Clinical Investigation, Inc.
Volume 84, December 1989, 1967–1973

attendant filtration deficit. More definitive information can be obtained in studies of glomerular dynamics.

Glomerular dynamic studies have been performed in the first 2–3 h after uranium injection (8) and in rats subjected to partial renal ischemia (9), cisplatin (10), or gentamicin poisoning (11) with widely divergent findings. In each case, moreover, the animals exhibited only a moderate filtration deficit, and it is unclear whether other mechanisms would have to be superimposed to yield the vanishingly low inulin clearance expected in fully established renal failure. Current views on the role and nature of altered glomerular dynamics in fully established ARF are based largely on studies of high-dose mercury (12) and prolonged total renal ischemia (7, 8), but failed filtration in these two models appears to be caused by entirely different mechanisms. The former is directly attributable to combined preglomerular vasoconstriction and postglomerular vascular relaxation with no necessary change in glomerular permeability, tubular obstruction, or leakage of filtrate (12). Glomerular capillary hydraulic pressure (P_g) is reduced to a degree that makes ongoing filtration impossible (12); Bowman's space (P_{BS}) (12) and proximal tubule (P_t) (13) pressures are not substantially raised. As manifest by a remarkably raised proximal tubule pressure, the latter model, by contrast, appears to be initiated by overt tubular obstruction, P_g actually being raised substantively above its normal value due to a presumed decrease in preglomerular resistance (14). Capillary pressure falls some 24 h later but can be raised again by saline infusion (14). Leakage or intratubular sequestration of much of the inulin filtered has been reported to play a prominent role (6). Which of the two models more closely emulates the mechanisms operative in human ARF is not clear and, especially since most instances of renal failure in man are not preceded by either prolonged total ischemia or mercury poisoning, the glomerular dynamics of other models deserve close scrutiny.

Glycerol-induced myohemoglobinuric ARF has many of the features of the "crush syndrome" in man, and hypertonic glycerol infusions have been reported to cause hemoglobinuric renal failure in human subjects (15). As in the human syndrome, this ARF model yields near total renal failure (5, 16–18) from which the rats recover spontaneously after some 5–7 d (19). The pathogenetic features and natural history of this model have been well characterized in previous studies (e.g., 5, 16–19), but the mechanisms immediately responsible for the apparent filtration deficit thus far have not been examined. The present report describes the glomerular dynamic abnormalities responsible for failed filtration in this murine ARF model.

Methods

Studies were performed on female Munich-Wistar rats weighing 156–182 g (Simonsen Laboratories, Gilroy, CA). The rats were

weighed and deprived of water overnight. Some 16 h later, 10 ml/kg body weight (BW) of 50% glycerol solution was injected intramuscularly in divided dosage into the two hind limbs (5). All animals were allowed free access to water thereafter, and studies were begun 18–26 h after glycerol injection.

The rats were anesthetized with 50 mg/kg BW pentobarbital i.p. and placed on a thermostatically regulated heating table controlled by a rectal thermistor and relay system (model 73A; Yellow Springs Instrument, Co., Yellow Springs, OH) to maintain body temperature at 37°C. A tracheostomy was performed and an indwelling silastic bladder catheter was placed per urethram. A femoral artery was cannulated for blood pressure measurement with a transducer (model 23 Gb; Statham-Gould, Hato Rey, Puerto Rico) attached to an electrometer (model 2202; Gould Inc., Cleveland, OH). The left femoral vein was cannulated and a volume of 150 mM NaCl or 5% dextrose solution equivalent to any weight loss remaining from the dehydration period was infused slowly. The infusion was followed by 2 ml of plasma from either normal donors (controls) or identically treated ARF blood donors (ARF rats) to replace surgical fluid loss. Depending on the protocol, the rats received either 2 μ Ci (nonmicropuncture) or 40 μ Ci (micropuncture experiments) [14 C]inulin in 1 ml 150 mM saline. The same solution was infused at a rate of 2.2 ml/h in normal controls but, because of the very low glomerular filtration rate, inulin was omitted from the maintenance infusion of ARF rats.

Studies of glomerular dynamics. Animals were prepared as described above. The left kidney was exposed through an abdomino-flank incision and placed in a lucite cup. Cool setting agarose was poured around the kidney to minimize respiratory movement (20), and the kidney was covered with warm saline. A 0.2-ml blood sample was obtained for triplicate measurement of arterial plasma colloid osmotic pressure (COP_A) using a membrane osmometer (model 3A; Instrumentation for Physiology & Medicine, San Diego, CA).

The kidney surface of each ARF rat was examined under the dissecting microscope at low magnification to catalogue the proportion of open vs. collapsed tubules. The flow of small droplets of 1 centistoke (cs) viscosity (i.e., the viscosity of H_2O) stained silicone oil injected into multiple fluid-filled proximal tubules was assessed as absent, slow, or brisk in multiple open tubules of each rat. The proximal tubule transit time (21) was determined after bolus intravenous injection of 0.05 ml 5% lissamine green (LG). Single nephron glomerular filtration rate (SNGFR) was measured directly by timed, quantitative fluid collection from the glomerulo-tubular junction (GTJ) of nephrons with surface glomeruli, as described previously (12). Since filtrate collected at the GTJ is not subject to tubular absorption, the SNGFR was considered equal to the timed collection rate. This approach, which permits the measurement of SNGFR uninfluenced by the possibility of inulin leakage, has been validated previously in normal and mercury-poisoned ARF rats (12). The volume of filtrate collected was measured in precalibrated 140 μ m i.d. constant bore capillary tubes (Drummond Scientific Co., Broomall, PA) with a microscope and filar eyepiece. SNGFR also was determined as the [14 C]inulin clearance measured in randomly selected open tubules by injecting a segment of 1 cs silicone oil, 3–4 lumen diameters in length, to isolate the puncture site from more distal nephron segments. Fluid then was collected quantitatively at a rate that held the oil segment motionless over an accurately timed period of up to 6 min. Plasma samples were obtained for measurement of [14 C]inulin activity immediately after each collection, and the SNGFR was calculated from the urine/plasma ^{14}C activity ratio and the fluid collection rate.

P_g , P_{BS} , P_t , and star vessel (P_{star}) pressures were measured with a servo-nulling capacitance device (David Smith Co., Chapel Hill, NC) using 1–2 μ m o.d. tip platinized pipettes filled with 2 M NaCl, as described elsewhere (20). The pipette holder was attached to a stepping drive (David Kopf Co., Tujunga, CA), which permitted the adjustment of tip placement micrometer by micrometer (20). P_g values were considered acceptable only if the pressure obtained was entirely constant for at least 1 min and if the contour of each wave form was detailed and identical from complex to complex (21). The pressure drop across the

preglomerular vascular resistance (R_A) was estimated as $(MAP - P_g)$. Since star vessels could rarely be identified with their parent glomeruli, $(P_g - P_{star})$ was estimated from individual P_g values and mean P_{star} for the kidney under study. COP_A measurement was repeated on completing each study.

To obtain a more extensive (albeit indirect) sampling than that available from the few surface glomeruli of each kidney, P_g also was derived from the stop flow pressure (P_{sf}) as described elsewhere (12). It was assumed that this technique would exert little effect on tubuloglomerular feedback in nephrons with scant filtration and that the otherwise expected rise in P_g secondary to stopped filtration and the resultant increased flow across postglomerular vascular resistance (R_E) (22, 23) would be very small. A 1–2- μ m-o.d. pressure pipette was inserted at the measurement site and a 10- μ m-o.d. pressure pipette containing 100,000 cs viscosity silicone oil was inserted more distally. P_{BS} or P_t was measured before occluding the tubule lumen with oil and thereafter until a stable pressure was reached. In normal rats, oil of this viscosity could not be injected rapidly enough to occlude the lumen and flowed away before tubular blockade could be attained. Since a wax injection system was not at hand, P_{sf} was not measured in controls.

In preliminary studies, the single nephron filtration fraction (SNFF) in six representative ARF rats was determined to establish the degree of variation within individual kidneys. SNFF was estimated from the activity of ^{125}I -labeled BSA, prepared and screened as described previously (24), in arterial (I^*_A) and star vessel (I^*_E) plasma. Star vessel blood samples were obtained with silicone-filled 12–14- μ m-o.d. pipettes with due care not to distort the vessel at the insertion site. While gentle aspiration often was needed to begin the collection and at times to restart a stopped collection, star vessel blood for the most part was collected without aspiration. An arterial blood sample was obtained immediately after each collection. After centrifugation, triplicate aliquots of arterial plasma and the entire star vessel sample were measured in 140- μ m-i.d. constant bore capillary tubes, as above. ^{125}I activity was determined in a gamma scintillation counter (LKB Instruments, Inc., Wallac, Turku, Finland). The filtration fraction was estimated as $SNFF = (1 - I^*_A/I^*_E)$.

Renal blood flow measurements. Renal cortical blood flow (CBF) was measured in a separate series of 10 volume-replete, glycerol-injected rats and 10 normal-control animals using the hydrogen washout technique (25, 26). This method, validated elsewhere (12, 27), correlates well with direct whole kidney blood flow measurements in both normal animals and rats with various forms of ARF (12, 27). The left kidney was exposed through an abdomino-flank incision, and three or four 100- μ m-diam, enamel-insulated platinum electrodes (Sigmund Cohn Co., Mt. Vernon, NY) with the distal 1–2 mm scraped and sharpened were inserted at widely separated sites in the outer 1 mm of cortex parallel to the kidney surface (27). The incision was closed around the electrodes, and C_{in} and CBF measurements were begun 30 min later. About 5% H_2 in air was administered via an open nose cone, and its activity in cortical tissue around the electrodes was measured with a differential amplifier connected to a Tecmar analog/digital converter (Scientific Solutions, Solon, OH) and a microcomputer (IBM Instruments, Inc., Danbury, CT). The hydrogen mixture was replaced with air when full-scale deflection was obtained, and measurements were begun 15–20 s later to avoid the effects of hydrogen recirculation. Any tracing that was not log-linear for at least two half-times ($t_{1/2}$) was discarded. CBF was calculated from the log-linearized H_2 washout curve as $0.693/t_{1/2}$ (26). Since the tissue/water partition coefficient for hydrogen is 1.0 in all tissues (28), no correction for H_2 distribution was required. The kidney was excised and weighed on completing blood flow measurements and, expressed as blood flow per gram cortex, CBF values for ARF rats were corrected for the increase in kidney weight relative to control, as described earlier (27). Plasma and quantitatively collected urine samples were obtained at the beginning and at two accurately timed 30–40-min intervals for C_{in} determinations, and CBF measurements were repeated during each period. In eight of these animals, whole kidney blood flow was measured using an electromagnetic square-wave system (Carolina Medical Electronics,

Table I. Micropuncture Data in Myohemoglobinuric and Control Rats

	MAP	P _g	COP _A	P _{BS}	P _{star}	ΔP _{netA}	SNGFR	GFR
		mmHg					nl/min	ml/min
Control (N = 11)								
Mean	115	49.6	15.1	13.8	14.1	19.9	30.6	1.7
SEM	1	1.6	0.8	1.1	0.5	1.7	1.2	0.1
n	11	40	11	45	33	40	36	11
ARF (N = 32)								
Mean	116	35.8*	15.7	14.9	13.1	6.3*	5.8*	0.05
SEM	2	0.8	1.0	0.4	1.0	1.2	1.1	0.01
n	32	42	32	42	42	42	42	23

Values shown for ARF rats are those for 42 nephrons in which all measured parameters were obtained concomitantly. See text for randomly obtained values. N = number of rats, and n = numbers of samples. * Significant difference from control at P < 0.001. All other values are not significantly different from control.

Inc., King, NC) with 2.5-mm inner circumference flow probes applied to the left renal artery.

Statistical analyses were performed according to Snedecor and Cochran (29). All means are presented ± 1 SEM, and comparisons between means used the unpaired or, where stated, paired t test.

Results

Micropuncture studies. Viewed under the dissecting microscope in vivo, approximately one-half (range 10–90%) of the surface nephrons of 47 ARF rats were devoid of fluid and totally collapsed. As judged from the flow rate of injected 1-cs silicone oil droplets, most of the fluid-filled tubules had greatly reduced or virtually no flow. The minimum mean proximal tubule LG transit time (LGTT), when measurable at all, was 50.8 ± 2.8 s (n = 20 rats), over four times longer than control (P < 0.001). LG appeared in only a small minority of nephrons, and LGTT could not be assessed in most of these because of inordinately slow axial flow and pale coloration of the tubule fluid. The normal marked deepening of color along the proximal tubule was rarely observed.

Measured at the GTJ of 42 fluid-filled nephrons in which values for P_g, SNGFR, and P_{BS} were obtained concomitantly, SNGFR in 32 rats averaged 5.8 ± SEM 1.1 nl/min, far lower than the control value of 30.6 ± 1.2 nl/min (Table I). The mean was distinctly raised by the few nephrons with near normal filtration (Fig. 1). Volumes adequate for measurement could not be obtained from the GTJ of 10 of these nephrons (or from any collapsed tubules) despite prolonged collection times of up to > 5 min. P_{BS} in these same 42 nephrons averaged 14.9 ± 0.4 mmHg, a value not different from 13.8 ± 1.1 mmHg in controls (P > 0.3). As shown in Fig. 2, there was no correlation between P_{BS} and SNGFR (r = 0.169, P > 0.2). COP_A was 15.7 ± 1 mmHg (control 15.1 ± 0.8 mmHg, NS), and the arterial hematocrit of 37 ± 1 ml/dl blood was 8 ml/dl lower than control (45 ± 0.7, P < 0.001). Mean P_g was 35.8 ± 0.8 mmHg, 14 mmHg below the control value of 49.6 ± 1.6 mmHg (P < 0.001). Mean afferent net filtration pressure (ΔP_{netA}) of 6.3 ± 1.2 nl/min in these fluid-filled nephrons was far below the control value of 19.9 ± 1.7 mmHg (P < 0.001). As shown in Fig. 1, SNGFR correlated well with ΔP_{netA} (y = 0.543x + 2.636, r = 0.678, P < 0.001). Despite the markedly depressed P_g, P_{star} averaged

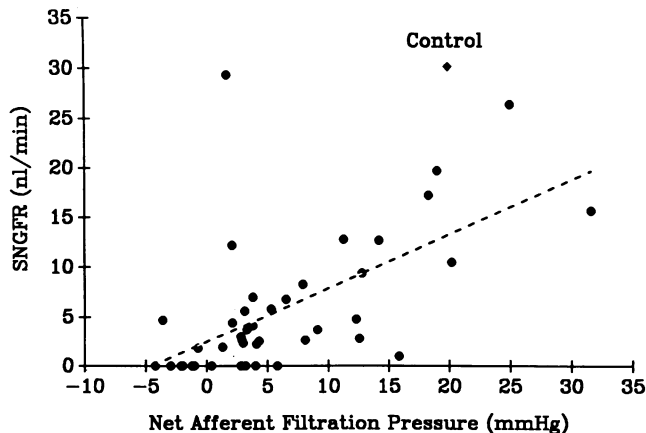


Figure 1. SNGFR as a function of ΔP_{netA} in rats with glycerol-induced acute renal failure. The control relationship between mean SNGFR and ΔP_{netA} is symbolized by a solid diamond while experimental values are depicted in closed circles. The least-squares regression line for the ARF rats is described by y = 0.543x + 2.636, r = 0.678, P < 0.001.

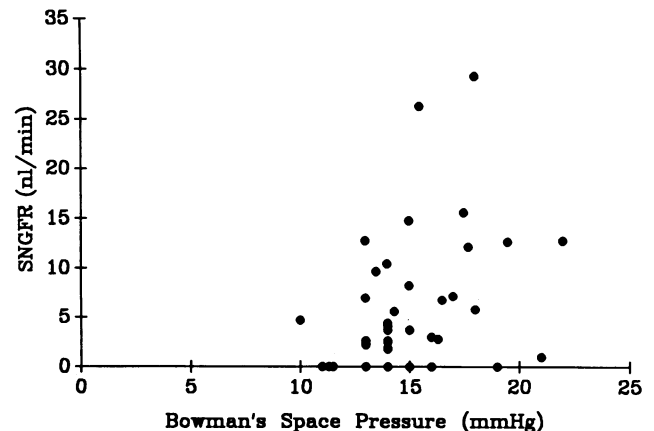


Figure 2. SNGFR as a function of P_{BS} in rats with acute renal failure. Although some individual values for P_{BS} were moderately elevated, the mean of 14.9 ± 0.4 mmHg was not statistically distinguishable from control. No correlation between P_{BS} and SNGFR was obtained (r = 0.169, P > 0.2).

13.1±1.0 mmHg, a value not statistically different from the control of 14.1±0.5 mmHg. (MAP - P_g) of individual rats averaged 79.5±3.5 mmHg, and (P_g - P_{star}) was 22.7±2.3 mmHg (controls 65.8±2.1 mmHg, $P < 0.001$, and 34.1±1.9 mmHg, $P < 0.001$), respectively. (MAP - P_g)/(P_g - P_{star}) averaged 3.5±0.3, far higher than 2.0±0.2 in controls ($P < 0.001$). With a normal SNFF of 0.29 (8, 13) in this rat substrain and a measured hematocrit (Hct) of 0.45 that yield an efferent/afferent glomerular blood flow ratio (GBF_E/GBF_A) of 0.81, the estimated, approximate R_A/R_E ratio in controls based on this (MAP - P_g)/(P_g - P_{star}) ratio was 1.6 (see Discussion for estimates of the R_A/R_E ratio in ARF rats).

Free-flow pressure in 14 nephrons used for stop-flow pressure (P_{sf}) measurements rose from 14.6±1.3 mmHg to a stable mean P_{BS} of 20.1±2.2 mmHg after tubule occlusion, an increase of 5.5±0.7 mmHg ($P < 0.001$ as paired data). P_{sf} was not measurable in controls with the technique employed (see Methods). With mean COP_A 15.4±1.5 mmHg in these animals, the estimated P_g of 35.6±1.5 mmHg was indistinguishable from that measured by capillary puncture in other nephrons (see above). Individual P_{sf} values correlated well with SNGFR obtained in the same nephrons ($y = 0.385x - 3.28$, $r = 0.585$, $P < 0.001$). P_t in 48 randomly selected fluid-filled proximal tubules was 13.8±0.8 mmHg and the proximal tubule P_{sf} was 18.3±1.2 mmHg, a rise of 5.4±0.9 mmHg. None of these values was statistically significantly different from those obtained in Bowman's space ($P > 0.1$ or higher). SNGFR in these same tubules averaged 5.4±1.3 nl/min, far lower than control ($P < 0.001$) but, again, not different from that obtained by glomerular puncture.

SNFF measured in six rats ($n = 18$) in preliminary studies was 0.11±0.01 with a range of -0.06-+0.21. None of the star vessels used for SNFF measurement could be identified with its parent glomerulus. In light of the wide variation in SNFF and the considerations outlined in Discussion, SNFF was not measured in the actual study.

Renocortical blood flow measurements. CBF in 10 normal control and 10 volume replete glycerol-injected animals not subjected to micropuncture was 6.9±0.2 and 6.5±0.6 ml/min·g cortex respectively, values which are not statistically significantly different. MAP, 113±2 mmHg, was not different from that of control animals (111±2 mmHg) during blood flow measurement or from the normal and ARF rats used for micropuncture (115±2 and 116±2 mmHg, respectively), and C_{in} of 0.03±0.05 ml/min was not different from that of rats used for glomerular dynamic studies. Whole kidney blood flow measured with the electromagnetic square-wave probe, 5.4±0.4 ml/min per kidney, was not distinguishable from the control value of 5.7±0.3 ml/min per kidney.

Discussion

Glycerol-induced myohemoglobinuric ARF shows many of the hallmarks of the "crush syndrome," the archetypical form of human acute renal failure that first led to the widespread recognition of this disorder in man (30). Injected intramuscularly, hypertonic glycerol causes myolysis, brisk hemolysis, and the sequestration of edema fluid at the injection site (5). Myoglobinuria and hemoglobinuria develop rapidly (5), the initial urine samples being deep port-wine in color. The C_{in} falls dramatically and renal cortical blood flow decreases to one-fourth of normal within 30 min of glycerol injection (26).

As confirmed in the present study, however, CBF returns to an essentially normal value within 24 h (27), while the GFR remains severely depressed until the onset of recovery some 5-7 d later (19). P_t falls markedly at the outset (5), rising subsequently to a near normal value and at no time showing the marked rise seen initially after renal artery clamping (6, 14) or uranium poisoning (8). The ultimate recovery of renal function reflects the progressive recruitment of increasing numbers of normally filtering nephrons rather than a gradual improvement in the function of the nephron population at large (19).

Prior volume depletion plays an important sensitizing role in this form of ARF. One-third of animals allowed free access to water before glycerol injection do not develop renal failure at all (16); volume depletion, by contrast, leads to consistently severe renal failure which persists even when the rats make up their initial water deficit by drinking (5, 16). Here, all rats were water-deprived before their ARF challenge but, in contrast to our previous micropuncture studies, any residual water deficit was replaced before micropuncture, and surgical fluid losses were restored with plasma. Although the hematocrit was decreased substantively due to active hemolysis, there was no discernible difference in plasma colloid osmotic pressure (Table I) to suggest the persistence of a reduced plasma volume. A contribution of ongoing volume depletion to the filtration deficit thus was ruled out.

The kidneys of these animals showed essentially the same changes found earlier in rats whose fluid deficit had not been systematically restored (e.g., 5, 16-18). Two populations of nephrons existed side by side, one fluid-filled and the other totally collapsed. The latter, in the majority, formed no filtrate at all. As determined by quantitative fluid collection at the GTJ of the few nephrons with surface glomeruli and the markedly prolonged LGTT, and slow axial flow of injected silicone droplets and low nephron C_{in} in the broader population, even the fluid-filled nephrons generally formed notably reduced volumes of filtrate. Renal failure thus reflected both the number of totally nonfunctioning nephrons and the degree to which filtration was impaired in the remainder. The finding of one superficial nephron that is filtering briskly surrounded by others that form virtually no filtrate, noted previously in this form of ARF (5, 16-19), suggests a local basis for filtration failure.

Major change in P_g in postischemic ARF follows a period of overt tubular obstruction (6, 7, 14). Mean P_{BS} was not raised in the present study, but even a normal pressure in nephrons with markedly reduced flow connotes an increased resistance to fluid outflow. Nonetheless, even those nephrons with the highest SNGFR did not exhibit a notably increased P_t, and there was no correlation between P_{BS} and SNGFR ($r = 0.169$, $P > 0.2$) to suggest that obstruction was essential to the development of filtration failure (Fig. 2). Moreover, serial studies of this ARF model from its onset to recovery have failed to demonstrate any period in which P_t is significantly increased (e.g., 5, 19). Thus, in contrast to the ischemic models (6, 7, 14) but in keeping with high-dose mercury poisoning (12), frank tubular obstruction is not an essential feature of failed filtration in myohemoglobinuric ARF.

Glomerular filtration is determined by the mean effective net filtration pressure, ΔP_{net} , and the glomerular ultrafiltration coefficient, K_f . In normal animals, a representative K_f value for each kidney is calculated from the mean SNGFR and ΔP_{net} , the latter in turn being derived from COP_A and the mean

values for COP_E , P_g , and P_{BS} . However, a star vessel used for COP_E measurement can rarely be identified with the parent nephron in which the other determinants are obtained. This poses no special problems in the normal kidney where internephron variation in COP_E and the various other measured parameters is not excessively large. Here, however, individual SNGFR values ranged from 0 to as high as 29.3 nl/min, while SNFF in preliminary experiments varied from some -0.1 to $+0.2$. Moreover, the SNFF estimate becomes exquisitely sensitive to small measurement errors as it approaches zero (12). Thus, with P_g also manifesting notable internephron variation, it was deemed inappropriate at the outset to pretend that combining these values from different nephrons would yield meaningful estimates of either ΔP_{net} or GBF_A . Without these parameters, definitive values for K_f and ΔP_{net} could not be derived. P_g and P_{BS} were measured in the same nephrons, however, and, when combined with COP_A , provided definitive values for the afferent effective net filtration pressure (ΔP_{netA}). The latter, reflecting a major fall in P_g , averaged some 14 mmHg lower than control.

P_g is the sole driving force for filtration and, at constant MAP and glomerular capillary resistance, is itself regulated by the R_A and R_E acting in concert. Values for these individual resistances normally are derived mathematically from the measured values for MAP, P_g , P_{star} , SNGFR and SNFF. Together with the arterial blood hematocrit, the latter two parameters are combined to yield GBF_A and GBF_E , which constitute the denominators of the resistance equations. For reasons given above, however, it was not possible to obtain definitive values for GBF_A and GBF_E and thus derive specific values for R_A and R_E in ARF rats. Nonetheless, with the normal whole-kidney blood flow and MAP values obtained in this study, it seems likely that blood flow to individual glomeruli (i.e., GBF_A), on average, was likewise not greatly changed. If so, the sum of the pre- and postglomerular resistances would have been essentially unaltered.

While GBF_A is determined by the sum of R_A and R_E , P_g (and thus the SNGFR) is an approximate function of the R_A/R_E ratio (12, 31). This ratio customarily is determined from the individual values for R_A and R_E , which are estimated separately as $R_A = (MAP - P_g)/GBF_A$ and $R_E = (P_g - P_{star})/GBF_E$. By combining and rearranging these equations, the R_A/R_E ratio can be estimated as: $R_A/R_E = (GBF_E/GBF_A) \cdot (MAP - P_g)/(P_g - P_{star})$. Although definitive values for GBF_A and GBF_E in ARF rats are not available (see above), we may assume limiting GBF_E/GBF_A ratios for individual nephrons of 1.0 ($GBF_E = GBF_A$, as in nonfiltering nephrons) and 0.86; the latter, at the mean hematocrit of 37 ml/dl found in ARF rats, corresponds to the highest-measured SNFF value of 0.21. Applying these boundary SNFF values to obtain putative maximum and minimum estimates of GBF_E/GBF_A and the measured values for MAP, P_g and P_{star} , the mean R_A/R_E ratio falls between 3.5 and 3.0. These values are some 2.2 and 1.9 times higher, respectively, than the control estimated

2. With P_g and P_{star} necessarily measured in different nephrons, there is some uncertainty in the calculated values for $(P_g - P_{star})$. However, P_{star} was far smaller than P_g and, unlike COP_E , varied little from nephron to nephron of a given kidney. Thus, the application of the mean P_{star} obtained for each animal to individual values for P_g should have introduced only a small and random error in the mean $(P_g - P_{star})$ estimate.

R_A/R_E ratio of 1.6 ± 0.2 , and the "true" value presumably falls toward the higher of these extremes. Accordingly, with the sum of R_A and R_E seemingly unchanged (see above) and the R_A/R_E ratio markedly increased, the low P_g in this ARF model appears to reflect an increase in R_A with a comparable fall in R_E rather than a change in either resistance alone. Assuming that GBF_A was indeed essentially unchanged, one may use simultaneous equations to calculate that R_A was some 23% higher than control while R_E , the smaller of the two resistances in the rat, fell by 38%. Taking vascular resistance to be a function of the fourth power of the radius, such changes correspond to a mere 5% decrease in the caliber of R_A and only a 13% increase in the radius of the efferent arteriole. If, by contrast, this doubling of the R_A/R_E ratio had been due exclusively to either a two-fold rise in R_A or a halving of R_E , there should have been a major change in P_{star} (22, 23) which simply was not observed. Thus, with P_g so markedly reduced and P_{star} indistinguishable from control, it seems necessary to invoke reciprocal changes in the two resistances even without the supposition that a normal cortical blood flow necessarily translates to a normal GBF_A .

Fig. 3, derived by network modeling (22) and the SPICE 2 simulation program (32), shows the SNGFR expected at different putative R_A/R_E ratios when applying the mean values for MAP, COP_A , Hct, and P_{BS} obtained here in rats with ARF (Table I). Assuming no alteration in total vascular resistance and a K_f unchanged from its normal control value of 2.2 nl/(min · mmHg) in this rat substrain (20), an R_A/R_E ratio of 3.25 (see above) yields a SNGFR that is entirely consistent with the mean value of 5.8 ± 1.1 nl/min obtained experimentally in the functioning nephron population. Only a minuscule additional change in R_A and/or R_E would be required to account for the total cessation of filtration manifest by the very large population of collapsed nephrons (see Fig. 3).

In editorial review, it was pointed out that the fall in postglomerular vascular resistance documented here might reflect reduced resistance of the more distal postglomerular vessels

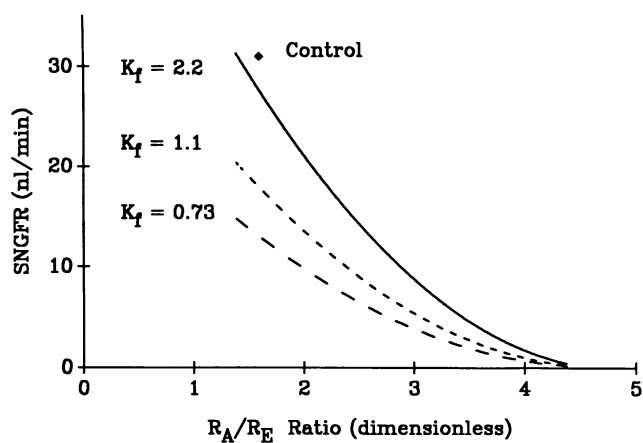


Figure 3. The nephron filtration rate (SNGFR) predicted by network thermodynamic modeling (22) at different assumed R_A/R_E ratios and with assumed ultrafiltration coefficients (K_f) of 2.2 (i.e., control), 1.1, and 0.73 nl · min/mmHg employing the measured values for MAP, P_{BS} , COP_A , and Hct_A of ARF rats. The control relationship is depicted with a solid diamond. The experimental mean R_A/R_E ratio in ARF rats was 3.5 ± 0.3 (dimensionless), at which value a reduction in the putative K_f to one-third of control exerts only a minimal additional effect on the SNGFR.

rather than the efferent arteriole itself. An inverse relationship between tubular and peritubular capillary diameters in normal rats has been reported by Jensen and Steven (33) and, indeed, as documented previously in this laboratory, the peritubular capillaries of collapsed nephrons of glycerol-injected rats do appear somewhat enlarged (5). However, the estimated control postefferent resistance (R_{PE}) in this substrain of Munich-Wistar rats is 0.05 mmHg · min/nl, while the sum of $R_E + R_{PE}$ is 0.28 mmHg · min/nl (20, 23). Accordingly, even a 50% solitary reduction in R_{PE} would reduce the total postglomerular resistance by only some 9%, far less than the actual reduction of 38% (see above). Although such a fall in peritubular capillary resistance, if present, would contribute somewhat to the overall resistance change, it still seems necessary to invoke efferent arteriolar relaxation as the key component of the lowered postglomerular resistance found in this form of ARF.

The root cause of the reciprocal resistance changes found here is unknown. To our knowledge, no vasoactive agonist except (possibly) adenosine (34) has been found to cause preglomerular vasoconstriction and concomitant efferent arteriolar relaxation in normal rats. The adenosine receptor blockers, aminophylline and 8-phenyltheophylline, have been reported to ameliorate glycerol-induced ARF in the rat to some degree (35, 36), presumably through their effects on glomerular dynamics. In our hands, these agents have provided only minor and inconsistent protection (37). A new and extremely potent adenosine receptor blocker, BW A1433U, did appear to totally protect glomerular filtration in initial experiments (37), but, for reasons that are entirely unclear, we have been unable to confirm that salutary effect in subsequent studies (unpublished data). While this does not rule out a possible role of adenosine as the mediator of the resistance changes found here, a definitive pathogenetic role is not confirmed. Treatment with α - and β -adrenergic blockers, indomethacin, or verapamil in this laboratory has in no way decreased the severity of renal failure obtained after glycerol injection (unpublished observations). Long-term salt loading totally aborts the development of renal failure in this model (38), but biologically effective active or passive immunization against renin (39) and angiotensin (40), and treatment with angiotensin-converting enzyme (unpublished data) have all been of no discernible value. This form of renal failure is not mitigated in Brattleboro rats with complete central diabetes insipidus (41), making the antidiuretic hormone an unlikely suspect. In short, the mediator of the complex resistance changes found here remains elusive. Hopefully, however, the documentation of the pathogenetic features responsible for failed filtration may serve as a rational basis for the consideration of other or new vasoactive agents (e.g., endothelin) as they appear.

When measured at the GTJ, SNGFR estimates are uninfluenced by the possibility of leakage at more distal tubular sites. Accordingly, with SNGFR greatly reduced or unmeasurable in the vast majority of nephrons of ARF rats, it seems that renal function would be markedly impaired whether the tubule system is "leaky" or not. Nonetheless, the C_{in} of most animals (mean < 2% of control) was far lower than would be predicted even from the spectrum of SNGFR values found here. This dichotomy does suggest that tubular leakage may have contributed to the severity of renal failure, although it also might reflect inhomogeneous function in deep and superficial nephrons or inflation of the SNGFR values by nephron

venting, such as occurs in low-dose HgCl₂ poisoning (1). Distinguishing between these possibilities is not within the scope of this study and must await experiments specifically designed for that purpose.

Although the K_f could not be estimated, the regression equation relating the measured values of SNGFR and ΔP_{netA} in Fig. 1 ($y = 0.543x + 2.63$, $r = 0.612$, $P < 0.001$), when extrapolated to a normal ΔP_{netA} of 19.8 mmHg, suggests that the glomerular hydraulic permeability of the rats with ARF may have been depressed by as much as 40%. On the other hand, modeling shows that the mean SNGFR obtained in fluid-filled nephrons corresponds well to that expected with the calculated resistance values and a normal K_f (see above). Moreover, the slope of the regression line was very heavily weighted by the large number of nephrons in which ΔP_{netA} and SNGFR were extremely low (see Fig. 1), and quite small measurement errors in P_g introduce a substantial adverse effect on the accuracy of the ΔP_{netA} estimate as it approaches zero. It is notable, therefore, that SNGFR was remarkably well maintained in those nephrons with the highest ΔP_{netA} values. Actually, even a 40% reduction in K_f , by itself, would lower the SNGFR of the normal rat by a mere 10% (22, 31). When superimposed on an increased R_A/R_E ratio of the magnitude recorded, moreover, even larger reductions in K_f can have only a minimal adverse effect on filtration (reference 31 and Fig. 3). Thus, any change in K_f that might have been present would have been of decidedly secondary importance in this ARF model.

In sum, rats with glycerol-induced myohemoglobinuric ARF manifest marked heterogeneity of individual nephron function. While the majority of surface nephrons formed virtually no filtrate despite full-volume repletion, others did filter small, and occasionally normal, volumes. Measured at the GTJ, the filtration deficit of individual nephrons correlated well with the fall in P_g and ΔP_{netA} of the same nephron. This reduction in P_g in turn reflected a major increase in R_A and a reciprocal drop in R_E that left total renal blood flow virtually unchanged. Although tubular outflow resistance apparently was increased, P_{BS} of fluid-filled tubules was normal and should have contributed little to the overall filtration deficit. Full volume replacement did not uncover covert, major tubular obstruction such as has been reported in established post-ischemic ARF (6, 7, 14). Internephron heterogeneity precluded reasonable estimates of the K_f which thus may or may not have contributed somewhat to the very low C_{in} obtained. However, the marked rise in the R_A/R_E ratio and the resultant fall in P_g sufficed to cause most, if not all, of the marked reduction in SNGFR observed. Accordingly, failed filtration in glycerol-induced myohemoglobinuric ARF is caused primarily by intrarenal hemodynamic changes comparable to those found in high-dose mercury poisoning. Both forms of renal failure display pathogenetic mechanisms that are entirely distinct from those reported after prolonged total renal ischemia (6, 7, 14).

Acknowledgments

We thank Ms. Katherine M. Reilly for her technical assistance with the blood flow measurements.

These studies were supported by National Institute of Environmental Health Sciences grant ESO4238-02 and the Veterans Administration.

References

1. Flamenbaum, W., F. D. McDonald, G. F. DiBona, and D. E. Oken. 1971. Micropuncture study of renal tubular factors in low dose mercury poisoning. *Nephron*. 8:221-234.
2. Biber, T. U. L., M. Mylle, A. D. Baines, C. W. Gottschalk, J. R. Oliver, and M. C. MacDowell. 1968. A study by micropuncture and microdissection of acute renal damage in rats. *Am. J. Med.* 44:644-705.
3. Flamenbaum, W., M. L. Huddleston, J. S. McNeil, and R. J. Hamburger. 1974. Uranyl-nitrate-induced acute renal failure in the rat: micropuncture and renal hemodynamic studies. *Kidney Int.* 6:408-418.
4. Henry, L. N., C. F. Lane, and M. Kashgarian. 1968. Micropuncture studies of the pathophysiology of acute renal failure in the rat. *Lab. Invest.* 19:309-314.
5. Oken, D. E., M. L. Arce, and D. R. Wilson. 1966. Glycerol-induced hemoglobinuric acute renal failure in the rat. I. Micropuncture study of the development of oliguria. *J. Clin. Invest.* 45:724-735.
6. Tanner, G. A., K. L. Sloan, and S. Sophosan. 1973. Effects of renal artery occlusion on kidney function in the rat. *Kidney Int.* 4:377-389.
7. Conger, J. D., J. B. Robinette, and S. J. Guggenheim. 1981. Effect of acetylcholine on the early phase of reversible norepinephrine-induced acute renal failure. *Kidney Int.* 19:399-409.
8. Blantz, R. C. 1975. Mechanism of acute renal failure after uranyl nitrate. *J. Clin. Invest.* 55:621-635.
9. Daugharty, T. M., I. F. Ueki, P. F. Mercer, and B. M. Brenner. 1974. Dynamics of glomerular ultrafiltration in the rat. V. Response to ischemic injury. *J. Clin. Invest.* 53:105-116.
10. Winston, J. A., and R. Safirstein. 1985. Reduced renal blood flow in early cisplatin-induced acute renal failure in the rat. *Am. J. Physiol.* 249:(Renal Fluid Electrolyte Physiol. 18):F490-F496.
11. Schor, N., I. Ichikawa, H. G. Rennke, J. L. Troy, and B. M. Brenner. 1981. Pathophysiology of altered glomerular function in aminoglycoside-treated rats. *Kidney Int.* 19:288-296.
12. Wolfert, A. I., L. A. Laveri, K. M. Reilly, K. R. Oken, and D. E. Oken. 1987. Glomerular dynamics in mercury-induced acute renal failure. *Kidney Int.* 32:246-255.
13. Flanagan, W. J., and D. E. Oken. 1965. Renal micropuncture study of the development of amuria in the rat with mercury-induced acute renal failure. *J. Clin. Invest.* 44:449-457.
14. Arendshorst, W. J., W. F. Finn, and C. W. Gottschalk. 1975. Pathogenesis of acute renal failure following temporary renal ischemia in the rat. *Circ. Res.* 37:558-568.
15. Hagnevik, K., E. Gordon, L.-E. Lins, S. Wilhelmsson, and D. Forster. 1974. Glycerol-induced haemolysis with haemoglobinuria and acute renal failure: report of three cases. *Lancet.* i:75-77.
16. Thiel, G., D. R. Wilson, M. L. Arce, and D. E. Oken. 1967. Glycerol induced acute renal failure in the rat. II. The experimental model, predisposing factors and pathophysiologic features. *Nephron.* 4:276-297.
17. Thiel, G., F. D. McDonald, and D. E. Oken. 1970. Micropuncture studies of the basis for protection of renin depleted rats from glycerol induced acute renal failure. *Nephron.* 7:67-79.
18. Wilson, D. R., G. Thiel, M. L. Arce, and D. E. Oken. 1969. The role of concentrating mechanisms in the development of acute renal failure: micropuncture studies using diabetes insipidus rats. *Nephron.* 6:128-139.
19. Oken, D. E., G. F. DiBona, and F. D. McDonald. 1970. Micropuncture studies of the recovery phase of myohemoglobinuric acute renal failure in the rat. *J. Clin. Invest.* 49:730-737.
20. Oken, D. E., A. I. Wolfert, L. A. Laveri, and S. C. Choi. 1985. Effects of intraanimal nephron heterogeneity on studies of glomerular dynamics. *Kidney Int.* 27:871-878.
21. Steinhausen, M. 1963. Eine Methode zur Differenzierung proximaler und distaler Tubuli der Nierenrinde von Ratten in vivo und ihre Anwendung zur Bestimmung tubularer Stromungsgeschwindigkeiten. *Pfluegers Arch. Gesamte Physiol. Menschen Tiere.* 277:22-35.
22. Oken, D. E., S. R. Thomas, and D. C. Mikulecky. 1981. A network thermodynamic model of glomerular dynamics: application in the rat. *Kidney Int.* 19:359-373.
23. Oken, D. E. 1982. An analysis of glomerular dynamics in rat, dog and man. *Kidney Int.* 22:136-145.
24. Jackson, B., and D. E. Oken. 1982. Internephron heterogeneity of filtration fraction and disparity between protein- and hematocrit-derived values. *Kidney Int.* 21:309-315.
25. Aukland, K., B. F. Bower, and R. W. Berliner. 1964. Measurement of local blood flow with hydrogen gas. *Circ. Res.* 14:164-187.
26. Chedru, M. F., R. Baethke, and D. E. Oken. 1971. Renal cortical blood flow and glomerular filtration in methemoglobinuric acute renal failure. *Kidney Int.* 1:232-239.
27. Churchill, S., M. D. Zarlengo, J. F. Carvalho, M. N. Gottlieb, and D. E. Oken. 1977. Normal renal cortical blood flow in experimental acute renal failure. *Kidney Int.* 11:246-255.
28. Grollman, A. 1929. The solubility of gases in blood and body fluids. *J. Biol. Chem.* 82:317-325.
29. Snedecor, G. W., and W. G. Cochran. 1967. Statistical Methods. 6th ed. Iowa State University Press, Ames, IA.
30. Bywaters, E. G. L., and D. Beall. 1941. Crush injuries with impairment of renal function. *Br. Med. J.* 1:427-432.
31. Oken, D. E. 1983. Theoretical analysis of pathogenic mechanisms in experimental acute renal failure. *Kidney Int.* 24:16-26.
32. Nagel, L. W. 1975. SPICE 2: A computer program to simulate semiconductor circuits. ERL Memo No. ERL-M520. Electronics Research Laboratory, University of California, Berkeley, CA.
33. Jensen, P. K., and K. Steven. 1979. Influence of peritubular pressure on proximal tubular compliance and capillary diameter in the rat kidney. *Pfluegers Arch. Eur. J. Physiol.* 382:179-187.
34. Osswald, H., H. J. Schmitz, and O. Heidenreich. 1975. Adenosine response of the rat kidney after saline loading, sodium restriction and hemorrhagia. *Pfluegers Arch. Eur. J. Physiol.* 357:323-333.
35. Bidani, A. K., and P. C. Churchill. 1983. Aminophylline ameliorates glycerol-induced acute renal failure in rats. *Can. J. Physiol. Pharmacol.* 61:567-571.
36. Bowmer C. J., M. G. Collis, and M. S. Yates. 1986. Effect of the adenosine antagonist 8-phenyltheophylline on glycerol-induced acute renal failure in the rat. *Br. J. Pharmacol.* 88:205-212.
37. Oken, D. E., and K. M. Reilly. 1989. Total prevention of glycerol-induced acute renal failure (ARF) with an adenosine-receptor blocker. *Kidney Int.* 35:415. (Abstr.)
38. Thiel, G., F. D. McDonald, and D. E. Oken. 1970. Micropuncture studies of the basis for protection of renin-depleted rats from glycerol-induced acute renal failure. *Nephron.* 7:67-79.
39. Flamenbaum, W., T. A. Kotchen, and D. E. Oken. 1972. Effects of renin immunization on mercuric chloride and glycerol-induced renal failure. *Kidney Int.* 1:406-412.
40. Oken, D. E., S. C. Cotes, W. Flamenbaum, J. S. Powell-Jackson, and A. F. Lever. 1975. Active and passive immunization to angiotensin in experimental acute renal failure. *Kidney Int.* 7:12-18.
41. Wilson, D. R., G. Thiel, M. L. Arce, and D. E. Oken. 1969. The role of concentrating mechanisms in the development of acute renal failure: micropuncture studies using diabetes insipidus rats. *Nephron.* 6:128-139.